PROCEEDINGS OF SPIE

SPIEDigitalLibrary.org/conference-proceedings-of-spie

CCD and Hartmann-Shack wavefront sensor to analyse holographic lens resolution

Tomás Lloret, Víctor Navarro-Fuster, Marta Morales-Vidal, Manuel Ramírez, Andrés Márquez, et al.

Tomás Lloret, Víctor Navarro-Fuster, Marta Morales-Vidal, Manuel G. Ramírez, Andrés Márquez, Augusto Beléndez, Inmaculada Pascual, "CCD and Hartmann-Shack wavefront sensor to analyse holographic lens resolution," Proc. SPIE 12574, Holography: Advances and Modern Trends VIII, 125740Z (31 May 2023); doi: 10.1117/12.2665716

SPIE.

Event: SPIE Optics + Optoelectronics, 2023, Prague, Czech Republic

Best Student Paper Award

CCD and Hartmann-Shack wavefront sensor to analyze holographic lens resolution

Tomás Lloret[a], Víctor Navarro-Fuster[c], Marta Morales-Vidal[a,b], Manuel G. Ramírez[b], Andrés Márquez[b,c], Augusto Beléndez[b,c], and Inmaculada Pascual[a,b]

[a]Departamento de Óptica, Farmacología y Anatomía, Universidad de Alicante, Carretera San Vicente del Raspeig s/n, 03690 San Vicente del Raspeig, Spain
[b]Instituto Universitario de Física Aplicada a las Ciencias y las Tecnologías, Universidad de Alicante, Carretera San Vicente del Raspeig s/n, 03690 San Vicente del Raspeig, Spain
[c]Departamento de Física, Ingeniería de Sistemas y Teoría de la Señal, Universidad de Alicante, Carretera San Vicente del Raspeig s/n, 03690 San Vicente del Raspeig, Spain

ABSTRACT

Nowadays, the study and optimization of volume holographic lenses (HLs) stored in low-toxicity photopolymers have a great interest. HLs are now a component of optical imaging systems that are mostly used in head-mounted displays for virtual and augmented reality or as non-image systems in light deflectors and concentrators. One of the most important parameters used when working with imaging systems is the resolution of the optical system. In this work, the similarity between the object and image of negative asymmetrical HLs stored in a low-toxicity photopolymer named Biophotopol has been evaluated theoretically and experimentally. For this purpose, the resolution of the HLs was calculated using the Convolution Theorem. A USAF 1951 test was used as an object and the impulse responses of the HLs were obtained with two different sensors: CCD and Hartmann-Shack (HS) wavefront sensor. In addition, the resolution of the HLs has been obtained by two different methods: one using the Convolution Theorem, using both the CCD and the HS wavefront sensor, and the other by forming the USAF test image on the CCD sensor. Finally, a theoretical study of object-image similarity was carried out using the MSE (mean squared error) metric to evaluate the quantitative experimental results.

Keywords: holographic lenses, volume holography, resolution, convolution theorem

1. INTRODUCTION

Holographic optical elements (HOEs) are one of the most significant holographic applications. HOEs are important because they can replace complex, heavy, curved refractive optical elements with simple, light, and flat elements.[1,2] Two spatially overlapping coherent beams form an interference pattern, which HOEs store. This pattern produces a photonic structure capable of bending light in the desired direction. Due to the simplicity of coupling the element for any type of manipulation and the ability to multiplex two or more HOEs, a wide variety of functionalities can be assembled on a single substrate according to its high diffraction efficiency and narrow band frequency properties. Filters, credit cards, displays, couplers, projection, and storage systems use HOEs as basic optical components.[3–6] Holographic lenses (HLs) have changed as various industries, such as communications, photonics, and information processing, have progressed. HLs are now a component of optical imaging systems that are primarily used in head-mounted displays for virtual and augmented reality[7] or as non-imaging systems in baffles and light concentrators.[8] In these applications, the optical and image quality of HLs is very important. To this end, some authors have studied the resolution of HLs using the modulation transfer function (MTF),[9] the Fourier transform, or the study of some quality metrics.[10] The MTF does not provide complete information about the resolution of HLs, since it only provides information about the cutoff frequency in a region of the image. For that reason, studying the convolution of an object resolution test with the impulse response of the HLs is a good option in order not to lose part of the information.

Further author information: (Send correspondence to T.L.L)
T.L.L: E-mail: tomas.lloret@ua.es

Holography: Advances and Modern Trends VIII, edited by Antonio Fimia, Miroslav Hrabovský, Proc. of SPIE Vol. 12574, 125740Z
© 2023 SPIE · 0277-786X · doi: 10.1117/12.2665716

In this work, we have studied the resolution of HLs recorded on a low-toxicity recording photopolymer in asymmetric and negative focal length recordings. In previous work, we obtained the best-quality results for negative asymmetric HLs. We have obtained the convolution between the impulse response, obtained from a CCD sensor and a HS wavefront sensor, and a USAF object test.[11]

2. METHODS

2.1 Recording material

Volume phase transmission HLs were recorded in a Biophotopol photopolymer, a low-toxicity hydrophilic material made up of one or more monomers in a binder, an electron donor, and a dye sensitizer. In earlier works, the component concentrations of Biophotopol have been thoroughly investigated to make up optimal photopolymer layers with good optical responses for storing HLs. The photopolymer solution, with water as a solvent, is made up of sodium acrylate (NaAO) as a polymerizable monomer, triethanolamine (TEA) as a co-initiator and plasticizer, sodium salt of monophosphate 5'-riboflavin monophosphate (RF) as a dye (absorption maximum at 488 nm wavelength), and polyvinylalcohol (PVA) as a binder (Mw=130,000, degree of hydrolysis=87.7%). Initially, the solution was prepared with the amounts of each of the components shown in Table 1. The material is not sensitive to red light, and all the compounds are mixed with a conventional magnetic stirrer few minutes. The photopolymer solution is deposited by gravity on square glass slides (6.5 x 6.5 cm^2).

Table 1. Recording material composition quantities.

PVA (wt/V %)	**NaAO (wt/V %)**	**TEA (wt/V %)**	**RF (wt/V %)**
13.5	3.70	0.13	0.05

Once the solution has been deposited, the samples are left in an incubator (Climacell 111) with controlled humidity and temperature (Hr=60±5% and T=20±1^oC). When part of the water has evaporated (drying time approximately 24 hours) the "solid" thickness of the film is approximately 200 μm, at which point the recording stage can be performed.

2.2 Experimental setup

The experimental holographic setup used to obtain the wavefront can be seen in Figure 1. To illuminate the HLs, a 473 nm diode-pumped laser whose wavelength was close to the recording one (488 nm) was used together with a 633 nm He–Ne laser. The beam, after being spatially filtered, was placed at the reconstruction angle (θ_C) that matched the recording angle. The conjugate beam was used when the lenses evaluated were negative. The HL and L_2, separated by a distance $f'_{HL}+f'_L$ formed an afocal lens system, from which the collimated emerging beam ends up hitting the HS wavefront sensor. Once the wave aberration function is obtained, the impulse response (Amplitude Spread Function) can be obtained.

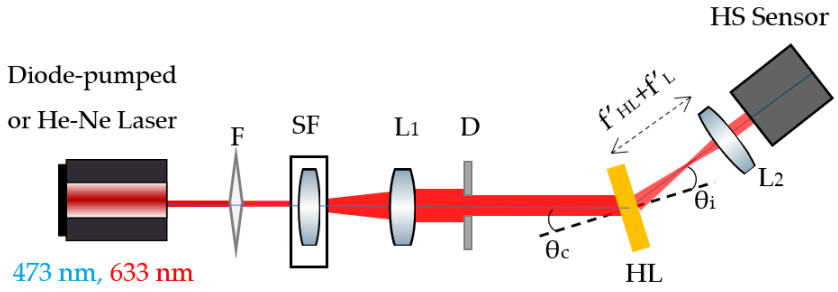

Figure 1. Experimental setup for the evaluation of the aberrated wavefront of holographic lenses. F: filter, SF: spatial filter, L: lens, D: diaphragm, HL: holographic lens, HS Sensor: Hartmann–Shack wavefront sensor.

3. THEORETICAL BACKGROUND

3.1 Convolution Theorem

Mathematically, a complex extended object can be represented as a weighted sum of impulse functions.[12] The impulse response of the HL studied is the ASF, which can be independent of the object plane position, in which case it is called invariant under translations. In addition, if there is no distortion in the system, the image plane coordinates are related linearly with the coordinates of the object plane through the lateral magnification M. Therefore, the image of an extended object can be calculated as an overlay of weighted ASF through the following direct operation.

$$I(x,y) = \int\int O(u,v) \cdot ASF\left(u - \frac{x}{M}, v - \frac{y}{m}\right) dudv \tag{1}$$

where $O(u,v)$ and $I(x,y)$ represent the object and the image, respectively. This integral is called *Convolution*. Therefore, the image of a complex object can be seen as a convolution of that object and the impulsive response of the system.

$$Image = Object \circledast ASF \tag{2}$$

3.2 Amplitude Spread Function (ASF)

The impulse response function describes the response of an imaging system to an object point and can be defined in amplitude or intensity. For an optical system working with coherent light, and whose pupil is circular, the impulse response is called the *Amplitude Spread Function* (ASF). On the other hand, when the light source is incoherent, this function is called the *Point Spread Function* (PSF) and represents the intensity distribution in the image plane. Moreover, for an aberration-free (diffraction-limited) system with a circular pupil, the PSF has an analytical solution and is the well-known *Airy's Disc*. Therefore, while for systems working with incoherent light, the impulse response is defined in intensity, for systems working with coherent light it is defined in amplitude.

Amplitude **Intensity**

$$P(u,v) = 2\left(\frac{J_1\left(2\pi\sqrt{u^2+v^2}R_{ps}\right)}{2\pi\sqrt{u^2+v^2}R_{ps}}\right) \qquad I(u,v) = \left|2\frac{J_1\left(2\pi\sqrt{u^2+v^2}R_{ps}\right)}{2\pi\sqrt{u^2+v^2}R_{ps}}\right|^2$$

where J_1 represents a first order Bessel function. In this work, we define the ASF obtained with a Hartmann-Shack wavefront sensor and that obtained with a CCD sensor.

3.2.1 Case 1: ASF obtained using a CCD sensor

In this case, to perform the convolution between the impulse response and an objective test, it is necessary to obtain the impulse response in complex amplitude, but this is not possible because when working with a CCD sensor only the impulse response in intensity can be obtained. A good option is to make an approximation and obtain the absolute value of the amplitude. According to previous work[9] the intensity in the image plane can be calculated as:

$$I(x',y';z') = \frac{1}{B^2}\left|\int\int_S A(x,y)exp\left[i\Delta(x,y;x',y';z')\right]dxdy\right|^2 \tag{3}$$

and the amplitude approximation can be obtained as

$$A(x',y';z') = \frac{1}{B}\left|\int\int_S A(x,y)exp\left[i\Delta(x,y;x',y';z')\right]dxdy\right| \tag{4}$$

so ASF can be considered to be $ASF(x',y';z') \approx A(x',y';z')$

3.2.2 Case 2: ASF obtained using a H-S wavefront sensor

On the other hand, the complex amplitude impulse response can be obtained using the Hartmann-Shack wavefront sensor. Aberrations can be defined in the exit pupil plane using the wavefront aberration function as

$$W(\rho,\theta) = \sum_{n=0,m=-n}^{k} \sum_{n-|m|=par}^{n} C_n^m \cdot Z_n^m(\rho,\theta) \tag{5}$$

where C_n^m are the Zernike coefficients which for negative asymmetric HL according to previous work[9,10] is dominated by spherical aberration (C_0^4) and $Z_n^m(\rho,\theta)$ is the general form given by

$$Z_n^m(\rho,\theta) = \begin{cases} N_n^m R_n^{|m|}(\rho)\cos(m\theta) & para \quad m \geq 0 \\ -N_n^m R_n^{|m|}(\rho)\sin(m\theta) & para \quad m < 0 \end{cases} \tag{6}$$

where the superscript m denotes the angular frequency, and the subscript n denotes the degree of the radial polynomial. In addition, the explicit form of the radial polynomial, $R_n^{|m|}$, is defined as

$$R_n^{|m|}(\rho) = \sum_{s=0}^{(n-|m|)/2} \frac{(-1)^s (n-s)!}{s![0.5(n+|m|)-s]![0.5(n-|m|)-s]!} \rho^{n-2s} \tag{7}$$

which is a polynomial of degree n containing the terms ρ_n, ρ_{n-2},..., ρ_m. It can also be deduced that the normalization factor, N_n^m , is defined as

$$N_n^m = \sqrt{\frac{2(n+1)}{1+\delta_{m0}}} \tag{8}$$

where δ_{m0} is the Kronecker delta.

Finally, the ASF is given as

$$ASF(x',y';z') = A \cdot FT\left[p(x',y') \cdot e^{-ik \cdot W(x',y')}\right]_{u=\frac{x'}{\lambda f'_{HL}}, v=\frac{y'}{\lambda f'_{HL}}} \tag{9}$$

where $x' = r\cos\theta$ and $y' = r\sin\theta$.

4. RESULTS AND DISCUSSION

A *USAF Test 1951* has been used to determine the resolution of an optical system to assess how closely an object and its image resemble one another when holographic lenses are utilized. The test consists of a succession of groups of three bars repeated in a pattern. They typically fall within the 0.25 to 228 lp/mm range. Each group has six components. The group is identified by a Group Number (-2, -1, 0, 1, 2, etc.), which is equivalent to 2 raised to the power of the first element's spatial frequency. Each element in the group is the sixth root of two units smaller than the element before it. The resolution of the system can be calculated using the equation or by reading the group and element number of the smallest pattern the optical system can resolve (using the condition of resolving at least 2 lines).

$$Resolution = 2^{Group+(Element-1)/6} \tag{10}$$

Convolution simulations of the USAF test with the *ASF* obtained by different methods were carried out. Figure 2 shows simulations of the convolution images between the USAF 1951 object test and the ASF obtained with the HS wavefront sensor, and figure 3 shows the same simulations but with the ASF obtained with the CCD sensor.

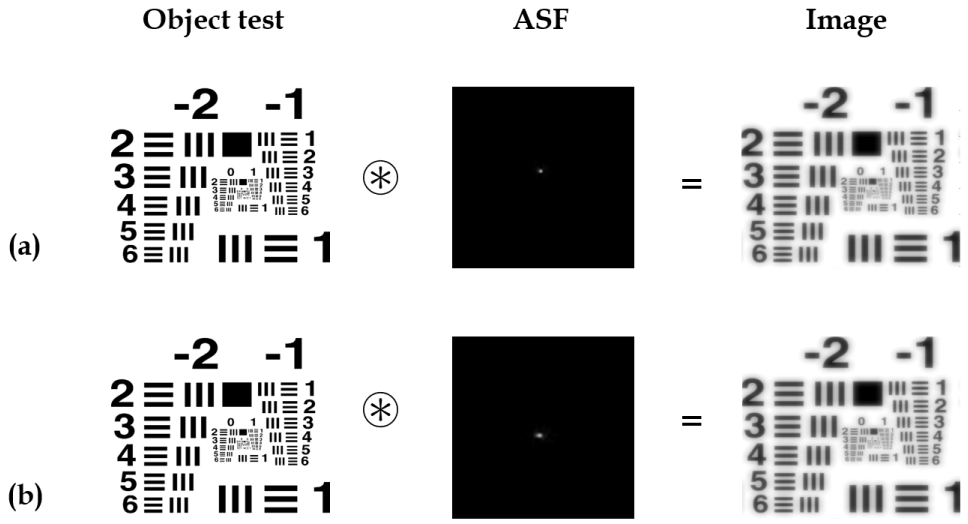

Figure 2. Simulated convolution for negative asymmetrical HLs, with ASF obtained with the HS wavefront sensor, reconstructed at (**a**) 473 nm and (**b**) 633 nm.

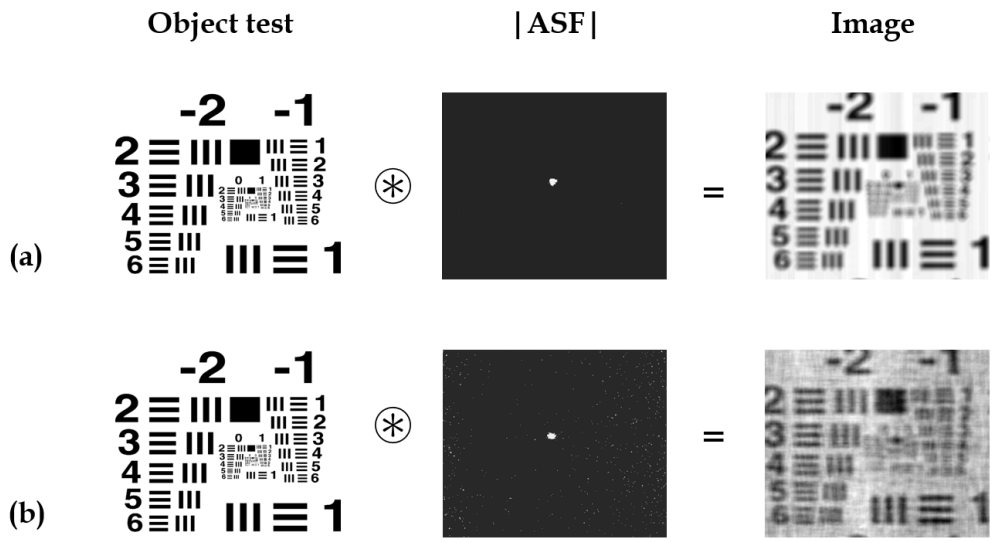

Figure 3. Simulated convolution for negative asymmetrical HLs, with ASF obtained with the CCD sensor, reconstructed at: (**a**) 473 nm, (**b**) 633 nm.

Table 2 shows the resolution of the holographic lens obtained in both methods for wavelengths 473 nm and 633 nm.

Table 2. Holographic lens resolution using the USAF test.

λ (nm)	**USAF H-S** (lp/mm)	**USAF CCD** (lp/mm)
473	11.31	4.00
633	11.31	3.17

5. CONCLUSIONS

We have studied two different methods to analyze the resolution of HLs stored in a photopolymer material (Biophotopol). In this sense, we have improved the way to measure this resolution. The resolutions obtained with the CCD sensor using the convolution theorem are less reliable than those obtained with the Hartmann Shack sensor. This is because part of the information is lost due to the way the HL impulse response is obtained in this case. The object-image similarity metric has also been analyzed to evaluate the HL resolution quantitatively. It can be observed that the best results have been obtained for the negative asymmetric HLs reconstructed at 473 nm. It can be concluded that the HS wavefront sensor is a good tool to characterize the image quality and resolution of optical systems working with coherent light using the convolution theorem. Moreover, the use of a low-toxicity photopolymer to store holographic lenses allows us to obtain light, friendly, accurate, stable, and easy-to-fabricate systems compared with traditional ones.

ACKNOWLEDGMENTS

This research was funded by Universidad de Alicante (UAFPU20-23); Generalitat Valenciana (CIDEXG/2022/60, IDIFEDER/2021/014, PROMETEO/2021/006); Ministerio de Ciencia e Innovación (PID2019-106601RB-I00, PID2021-123124OB-I00).

REFERENCES

[1] Schwar, M., Pandya, T., and Weinberg, F., "Point holograms as optical elements," *Nature* **215**, 239–241 (1967).

[2] Store, T. and Thompson, B., "Holographic and diffractive lenses and mirrors," *SPIE Milestore Ser.* **34**, 3–668 (1991).

[3] Piao, M., Kim, N., and Park, J., "Phase contrast projection display using photopolymer," *J. Opt. Soc. Korea* **12**, 319–325 (2008).

[4] Lee, K., Jeung, S., Cho, B., and Kim, N., "Photopolymer-based surface-normal input/output volume holographic grating coupler for 1550-nm optical wavelength," *J. Opt. Soc. Korea* **16**, 17–21 (2012).

[5] Fernández, E., Márquez, A., Gallego, S., Fuentes, R., García, C., and Pascual, I., "Hybrid ternary modulation applied to multiplexing holograms in photopolymers for data page storage," *J. Light. Technol.* **28**, 776–783 (2010).

[6] Sheridan, J., Kostuk, R.K.and Gil, A., Wang, Y., Lu, W., Zhong, H., Tomita, Y., Neipp, C., Francés, J., Gallego, S., and et al., "Roadmap on holography," *J. Opt.* **22**, 123002 (2020).

[7] Lin, W.-K., Matoba, O., Lin, B.-S., and Su, W.-C., "Astigmatism and deformation correction for a holographic head-mounted display with a wedge-shaped holographic waveguide," *Appl. Opt.* **57**, 7094–7101 (2018).

[8] Morales-Vidal, M., Lloret, T., Ramirez, M., Beléndez, A., and Pascual, I., "Green and wide acceptance angle solar concentrators," *Opt. Express* **30**, 25366–25379 (2022).

[9] Lloret, T., Navarro-Fuster, V., Ramirez, M., Ortuño, M., Neipp, C., Beléndez, A., and Pascual, I., "Holographic lenses in an environment-friendly photopolymer," *Polymers* **10(3)**, 302 (2018).

[10] Lloret, T., Navarro-Fuster, V., Ramirez, M., Morales-Vidal, M., Beléndez, A., and Pascual, I., "Aberration-based quality metrics in holographic lenses," *Polymers* **12(4)**, 993 (2020).

[11] Lloret, T., Morales-Vidal, M., Navarro-Fuster, V., Ramirez, M., Beléndez, A., and Pascual, I., "Holographic lens resolution using the convolution theorem," *Polymers* **14(24)**, 5426 (2022).

[12] Goodman, J., [*Introduction to Fourier optics*], Roberts and Company Publishers, Englewood, CO (2005).